Global Journal of Engineering and Technology Advances

eISSN: 2582-5003

Cross Ref DOI: 10.30574/gjeta

Journal homepage: https://gjeta.com/

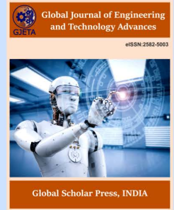

(Research Article)

ADC Histogram Test Using Triangular Stimulus Signals

Francisco André Corrêa Alegria *

Telecommunications Institute, Instituto Superior Técnico, University of Lisbon, Av. Rovisco Pais, 1, 1049 Lisbon, Portugal.

Global Journal of Engineering and Technology Advances, 2023, 16(03), 121–133

Publication history: Received on 26 July 2023; revised on 08 September 2023; accepted on 11 September 2023

Article DOI: https://doi.org/10.30574/gjeta.2023.16.3.0188

Abstract

This paper focuses on tackling the uncertainty in ADC testing estimates using the Histogram Method with a triangular stimulus instead of a sinusoidal one as is standard practice. It introduces expressions to calculate the standard deviation of transition voltages and code bin widths.

Keywords: Analog-to-Digital Converter; Histogram Method; Testing; Uncertainty; Noise

1. Introduction

Characterization of analog to digital converters (ADCs) involves several test methods, among which is the Histogram Test Method stands as one of the most widely utilized approaches for estimating the ADC transfer function [1]-[7]. Traditionally, this method has been employed with sinusoidal stimulus signals [8]-[9], as many other methods do [10]-[12], providing dynamic characterization of the converter. However, recent advances have led to the use of triangular waves for static testing of ADCs through a method known as "Ramp Vernier" [13]-[16].

In any measurement process, it is crucial to estimate not only the transition voltages and code bin widths of an ADC but also their associated uncertainties. This paper contributes to addressing this issue, focusing specifically on the case of using triangular stimulus signals in conjunction with the Histogram procedure. Previous research has been carried out on the bias of this test method, exploring optimal overdrive levels to minimize the impact of additive noise on the error of transition voltages and code bin widths [17].

The paper's structure is as follows: In Section 2, the Histogram test method is described, and the variables employed to describe the ADC transfer function and stimulus signal are introduced. Moving to Section 3, the variance of the transition voltages is computed, followed by the computation of the variance of the code bin widths in Section 4. Finally, Section 5 presents the conclusions drawn from the research.

Overall, this paper significantly contributes to the understanding of uncertainty estimation in ADC testing, particularly when employing triangular stimulus signals and the Histogram Test Method. This research opens up new possibilities for more accurate and reliable ADC characterizations, shedding light on potential improvements and optimizations in the testing process.

2. Histogram Test Method

The Histogram procedure [18] is a fundamental approach used in the characterization of analog to digital converters (ADCs). This method involves subjecting the ADC under test to acquire an extensive set of samples from a known input signal, typically a sinusoid. Subsequently, the digital codes corresponding to each of these samples are utilized to construct a cumulative histogram ($CH[k]$). The array $CH[k]$ represents the count of samples with digital codes equal to

* Corresponding author: Alegria, Francisco André Corrêa

Copyright © 2023 Author(s) retain the copyright of this article. This article is published under the terms of the Creative Commons Attribution Liscense 4.0.

or lower than each of the possible ADC output codes k. Essentially, it provides a distribution of how frequently different output codes occur in the ADC's response to the given input signal.

The cumulative histogram, $CH[k]$, is an array consisting of 2^N values, where N represents the number of bits of the ADC. Each value in the $CH[k]$ array corresponds to the number of samples whose digital code falls within the specific range defined by the ADC output codes. For instance, $CH[0]$ would indicate the number of samples with the lowest digital code (all 0s), $CH[1]$ would represent the number of samples with the next digital code (0001 in binary), and so on, up to $CH[2^N-1]$, which would represent the highest digital code (all 1s).

By analyzing the cumulative histogram, engineers and researchers can gain valuable insights into the behavior of the ADC, including its linearity, resolution, and potential non-idealities. The shape and characteristics of the histogram provide essential information about the ADC's transfer function, allowing for the estimation of critical parameters such as Differential Non-Linearity (DNL) and Integral Non-Linearity (INL).

Overall, the Histogram procedure serves as a crucial tool in ADC testing and characterization, enabling the evaluation of its performance and aiding in the identification of potential issues or optimizations in the conversion process. With this method, engineers can better understand the ADC's response to different input signals and ensure its accuracy and reliability in various applications.

From this array, the ADC transition voltages are estimated using

$$T[k] = 2A\frac{CH[k-1]}{M} - A \quad , \quad k = 1 \ldots 2^N - 1 \text{ ,............(1)}$$

and the code bin widths using

$$W[k] = 2A\frac{H[k]}{M} \quad , \quad k = 1 \ldots 2^N - 2 \text{ ,..........(2)}$$

where M is the number of samples and $H[k]$ is the number counts of the histogram which is the number of samples with each of the possible ADC output codes k. The relation between the value of the histogram and the cumulative histogram is

$$H[k] = CH[k] - CH[k-1] \quad , \quad k = 1 \ldots 2^N - 1 \text{ ....(3)}$$

In the traditional histogram method for ADC characterization, a full-scale periodic stimulus signal is applied to the ADC under test. This stimulus signal spans the entire input voltage range of the ADC and is applied continuously. Simultaneously, a specific number of samples are acquired from the ADC's output at a constant rate, but asynchronously with respect to the stimulus signal.

The crucial step in this method involves determining the ADC's transition voltages, which are the boundaries that separate different output codes. These transition voltages are essential for understanding the ADC's behavior, linearity, and resolution.

To obtain the ADC transition voltages, a comparison is made between the number of samples acquired in each code bin (ranges of output codes) and the number that would be expected in an ideal ADC. In an ideal ADC, the distribution of samples in each code bin would be perfectly uniform due to the uniform distribution of input voltages across the ADC's range.

To compute the expected number of samples in each code bin, knowledge of the probability distribution of the sample voltages is required. In other words, the value of the input signal at the precise moment of sampling needs to be known. This information is crucial to accurately estimate the expected distribution of samples in an ideal scenario.

However, in practice, the exact input signal value at the sampling instant is not always accessible, and this introduces uncertainty in the estimation of the ADC transition voltages. Various factors, such as noise [19], jitter [20], and non-idealities in the sampling process [21]-[24], can further contribute to this uncertainty. As a result, researchers and engineers often resort to statistical methods and multiple samples to improve the accuracy of the transition voltage estimation.

Overall, the traditional histogram method plays a fundamental role in ADC testing, as it allows engineers to analyze the ADC's performance and understand its response to the input stimulus. By estimating the transition voltages and evaluating the distribution of samples, valuable insights into the ADC's linearity and other important characteristics can be obtained, facilitating the optimization and refinement of ADC designs for various applications.

Consider each sample j ($j = 0, 1, \ldots, M - 1$) ideally acquired at instant t_j. Without loss of generality the time origin can be set to the ideal sampling instant of the first sample ($t_0 = 0$). The phase of the samples (γ_j), relative to the stimulus signal of frequency f, is thus

$$\gamma_j = 2\pi f \cdot t_j + \varphi \quad \text{……………(4)}$$

where φ represents the phase of the stimulus signal at the ideal instant of acquisition of the first sample. The value of the sinusoidal stimulus signal in the sampling instant of sample j can be written as

$$x_j = d - A \cdot \mathrm{tri}\left(2\pi f \cdot t_j + \varphi\right) \quad \text{……………..(5)}$$

where d and A are the stimulus signal offset and amplitude. The "tri(x)" function represents a general triangular wave function spanning from $-\pi$ to π in x and from -1 to 1 in amplitude:

$$\mathrm{tri}(x) = \begin{cases} 1 - 4\left\langle \dfrac{x}{2\pi} \right\rangle & , 0 < \left\langle \dfrac{x}{2\pi} \right\rangle \leq \dfrac{1}{2} \\ 4\left\langle \dfrac{x}{2\pi} \right\rangle - 3 & , \dfrac{1}{2} < \left\langle \dfrac{x}{2\pi} \right\rangle < 1. \end{cases} \quad \text{…………………(6)}$$

The values of the sampled voltages (v_j) are equal to the value of the stimulus signal in the sampling instant (x_j) plus the input-equivalent wideband noise (n_v).

$$v_j = n_v + d - A \cdot \mathrm{tri}\left(2\pi f \cdot t_j + \varphi\right) \quad \text{…………………(7)}$$

To simplify the computations, some normalizations are made. Let u_j be the normalized sample voltage.

$$u_j = \frac{v_j - d}{A} = \frac{n_v}{A} - \mathrm{tri}\left(\gamma_j\right) = n - \mathrm{tri}\left(\gamma_j\right) \quad \text{…………………..(8)}$$

where n is the normalized input-equivalent wideband noise and γ_j is the sample phase.

Next, we will focus on the estimation of the transition voltages made from the cumulative histogram array.

3. Variance of the Transition Voltages

3.1. General sampling

This section introduces the calculation of the probability distribution for the number of counts in the histogram, considering a general type of sampling, whether it is random, synchronous, or asynchronous. The subsequent section will focus on the specific scenario of asynchronous sampling.

Moreover, taking into account that the input-equivalent noise follows a normal distribution with a mean of zero and a standard deviation denoted by σ_n, we can derive the probability density function (p.d.f.) of the sample voltages (u_j).

$$f_{u_j}\left(u \mid \gamma_j\right) = \frac{1}{\sqrt{2\pi}\sigma_n} e^{-j\frac{\left(u + tri\left(\gamma_j\right)\right)^2}{2\sigma_n^2}} \quad \text{………………(9)}$$

Figure 1 represents the probability that a sample belongs to a class of the cumulative histogram as a function of the sample phase (γ_j) and of the input-equivalent noise standard deviation (σ_n) for the case of $U[k+1] = 0$ (transition voltage equal to the DC value of the stimulus signal).

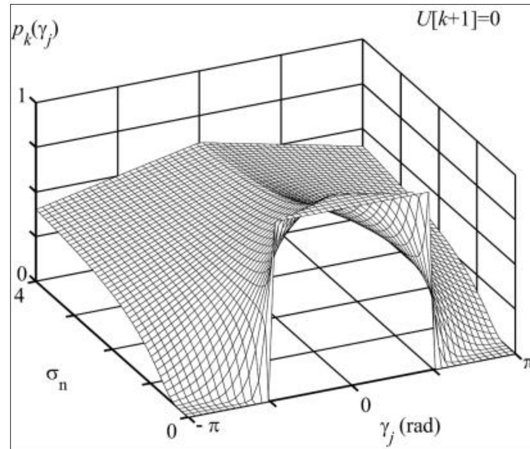

Figure 1 Representation of the probability that a sample belongs to a class of the cumulative histogram as a function of the sample phase (γ_j) and of the input-equivalent noise standard deviation (σ_n). Example with $U[k+1]=0$ (transition voltage equal to the DC value of the stimulus signal)

The probability that a sample j belongs to a class k of the cumulative histogram (p_k) is equal to the probability that the normalized sample voltage is between normalized transition voltage $U[k]$ and $U[k+1]$:

$$p_k(\gamma_j) = \int_{-\infty}^{U[k+1]} f_{u_j}(u \mid \gamma_j) \cdot du = \frac{1}{2} + \frac{1}{2} erf\left(\frac{U[k+1] + tri(\gamma_j)}{\sqrt{2} \cdot \sigma_n} \right) \quad \text{.............(10)}$$

Consider now a variable w_k that takes the value 1 if a sample belongs to class k of the cumulative histogram and 0 if not.

$$f_{w_k}(w \mid \gamma_j) = \begin{cases} p_k(\gamma_j) & , \ w = 1 \\ 1 - p_k(\gamma_j) & , \ w = 0 \end{cases} \quad \text{.......(11)}$$

This variable has a binomial distribution with mean pk and variance $p_k \cdot (1 - p_k)$. The number of counts in class k of the histogram (c_k) is the sum of variable w_k for all the samples. The p.d.f. of c_k is the convolution of the p.d.f. of the M variables w_k, because they are independent.

$$f_{c_k}(c \mid \varphi) = f_{w_k}(w \mid \gamma_0) * \ldots * f_{w_k}(w \mid \gamma_{M-1})(c) \quad \text{..................(12)}$$

Note that now, the p.d.f. of the number of counts is conditional to the initial phase φ and not to the sampling instant γ_j. The conditional mean of c_k is the sum of the conditional means of the variables w_k for each sample. The same is true for the conditional variance.

The total p.d.f. of the number of counts can be obtained by integrating the product of the conditional p.d.f. with the p.d.f. of the initial stimulus signal phase (f_φ) [25].

$$f_{c_k}(c) = \int_{-\infty}^{\infty} f_{c_k}(c \mid \varphi) \cdot f_\varphi(\varphi) \cdot d\varphi \quad \text{............(13)}$$

From the total p.d.f. $f_{c_k}(c)$, it is possible to determine the total mean,

$$\mu_{c_k} = \int_{-\infty}^{\infty} \mu_{c_k|\varphi} \cdot f_\varphi(\varphi) \cdot d\varphi \quad \text{..........(14)}$$

and variance of the number of counts:

$$\sigma_{c_k}^2 = \int_{-\infty}^{\infty} \sigma_{c_k|\varphi}^2 f_\varphi(\varphi) d\varphi + \int_{-\infty}^{\infty} \mu_{c_k|\varphi}^2 f_\varphi(\varphi) d\varphi - \left[\int_{-\infty}^{\infty} \mu_{c_k|\varphi} f_\varphi(\varphi) d\varphi \right]^2 \quad \text{.............(15)}$$

3.2. Asynchronous sampling

Now, let's take into account that the sampling process is carried out asynchronously with respect to the stimulus signal, meaning that the initial phase of the stimulus signal is not under control. In this context, we consider that this initial phase follows a uniform distribution, spanning from 0 to 2π.

Additionally, if the frequencies of both the sampling clock and the stimulus signal are chosen deliberately and are not harmonically related to each other, a desirable outcome is achieved. Specifically, the ideal sample phases become uniformly spaced. This alignment of ideal sample phases provides a favorable condition for accurate and reliable measurements during the asynchronous sampling procedure.

The ideal sample phases are uniformly spaced:

$$\gamma_j = j\frac{2\pi}{M} + \varphi \quad \text{...............(16)}$$

With some manipulation an expression for the mean

$$\mu_{c_k} = \frac{M}{2\pi} \int_{-\pi}^{\pi} p_k(\gamma) d\gamma \quad \text{...............(17)}$$

and for the variance

$$\sigma_{c_k}^2 = \mu_{\sigma_{c_k|\varphi}^2} + \sigma_{\mu_{c_k|\varphi}}^2$$

$$\mu_{\sigma_{c_k|\varphi}^2} = \frac{M}{2\pi} \int_{-\pi}^{\pi} p_k(\gamma)\left[1 - p_k(\gamma)\right] d\gamma$$

$$\sigma_{\mu_{c_k|\varphi}}^2 = \frac{M}{2\pi} \int_{0}^{\frac{2\cdot\pi}{M}} \left(\sum_{j=0}^{M-1} p_k\left(j\frac{2\pi}{M} + \varphi \right) \right)^2 d\varphi - \left(\frac{M}{2\pi} \int_{-\pi}^{\pi} p_k(\gamma) d\gamma \right)^2 \quad \text{.......... (18)}$$

can be easily derived from (15), (16) and (17). These expressions are written in terms of the number of samples acquired (M) and the probability that a sample belongs to a class of the cumulative histogram (p_k). The value of this probability depends, in turn, on the normalized input-equivalent noise standard deviation (σ_n), on the normalized transition voltage ($U[k]$) and sample phase (γ_j).

The expression for the variance was divided into two terms: the mean of the conditional variance ($\mu_{\sigma_{c_k|\varphi}^2}$) and the variance of the conditional mean ($\sigma_{\mu_{c_k|\varphi}}^2$).

3.3. Mean of the conditional variance

In this paragraph we analyse the mean of the conditional variance. Inserting (10) into (18) leads to

$$\mu_{\sigma_{c_k|\varphi}^2} = \frac{M}{2\pi} \cdot \int_{-\pi}^{\pi} \frac{1}{4} \cdot \left[1 - erf^2\left(\frac{U[k+1] + \mathrm{tri}(\varphi)}{\sqrt{2} \cdot \sigma_n} \right) \right] \cdot d\varphi \quad \text{.............(19)}$$

which is depicted in Figure 2.

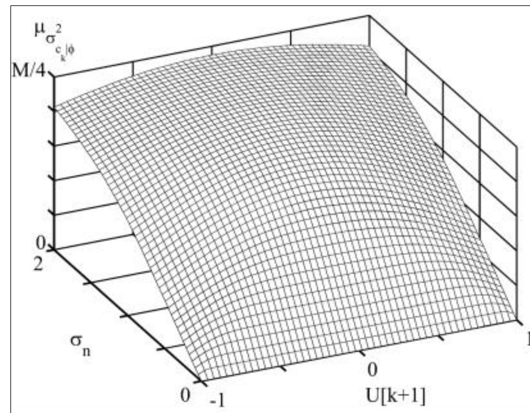

Figure 2 Representation of the term $\mu_{\sigma^2_{c_k|\varphi}}$ as a function of the standard deviation of the input-equivalent noise (σ_n) and of the normalized transition voltage

The term $\mu_{\sigma^2_{c_k|\varphi}}$ of the variance of the number of counts of the histogram is maximum for a transition voltage equal to the stimulus signal offset ($U[k]$=0). Ideally this would be the middle of the ADC input range. In this case the dependence of $\mu_{\sigma^2_{c_k|\varphi}}$ on the standard deviations of input-equivalent noise is represented in Figure 3.

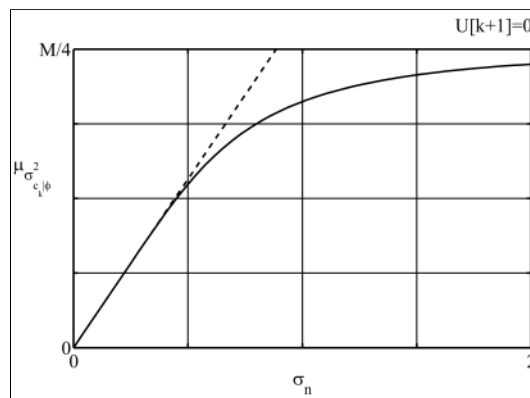

Figure 3 Representation of the term $\mu_{\sigma^2_{c_k|\varphi}}$ as a function of the standard deviation of the input-equivalent noise (σ_n) for a null value of normalized transition voltage. The dotted line represents the approximation for small values of input-equivalent noise standard deviation given by (27)

As the input-equivalent noise standard deviation goes to 0, the mean of the conditional variance is directly proportional to that same standard deviation. To prove that we will compute the following limit:

$$\lim_{\sigma_n \to 0} \frac{\mu_{\sigma^2_{c_k|\varphi}}}{\sigma_n} = \frac{M}{2\pi\sqrt{\pi}} \lim_{\sigma_n \to 0} \int_{-\pi}^{\pi} \frac{\sqrt{\pi}}{4\cdot\sigma_n} \cdot \left[1 - erf^2\left(\frac{U[k+1] + \mathrm{tri}(\varphi)}{\sqrt{2}\cdot\sigma_n}\right)\right] d\varphi \quad \text{............(20)}$$

Introducing now variable x:

$$x = U[k+1] + \mathrm{tri}(\varphi) \quad \text{..........(21)}$$

and inserting it into (20), leads to

$$\lim_{\sigma_n \to 0} \frac{\mu_{\sigma^2_{c_k|\varphi}}}{\sigma_n} = \frac{M}{\pi\sqrt{\pi}} \lim_{\sigma_n \to 0} \int_{U[k+1]-1}^{U[k+1]+1} \frac{\sqrt{\pi}}{4\cdot\sigma_n} \frac{\pi}{2}\left[1 - erf^2\left(\frac{x}{\sqrt{2}\cdot\sigma_n}\right)\right] \cdot dx \quad \text{...........(22)}$$

To obtain (22) we rewrote (21) as

$$\varphi = atri\left(x - U\left[k+1\right]\right) \quad \text{..........(23)}$$

The derivative is $\partial\varphi/\partial x = \pi/2$.

The limits of the integral in (22) can be extended to infinite for small values of σ_n:

$$\lim_{\sigma_n \to 0} \frac{\mu_{\sigma^2_{c_k|\varphi}}}{\sigma_n} = \frac{M}{\pi\sqrt{\pi}} \lim_{\sigma_n \to 0} \int_{-\infty}^{\infty} \frac{\sqrt{\pi}}{4\cdot\sigma_n} \frac{\pi}{2}\left[1 - erf^2\left(\frac{x}{\sqrt{2}\cdot\sigma_n}\right)\right]\cdot dx \quad \text{............(24)}$$

Considering that

$$\lim_{\sigma_n \to 0} \int_{-\infty}^{\infty} \frac{\sqrt{\pi}}{4\cdot\sigma_n}\left[1 - erf^2\left(\frac{x}{\sqrt{2}\cdot\sigma_n}\right)\right]\cdot dx = 1 \quad \text{............(25)}$$

we have

$$\lim_{\sigma_n \to 0} \frac{\mu_{\sigma^2_{c_k|\varphi}}}{\sigma_n} = \frac{M}{2\sqrt{\pi}} \quad \text{..................(26)}$$

which demonstrates that we can approximate the mean of the conditional variance by

$$\mu_{\sigma^2_{c_k|\varphi}} = \frac{M}{2\sqrt{\pi}}\sigma_n \quad \text{................(27)}$$

For large values of standard deviation, the term $\mu_{\sigma^2_{c_k|\varphi}}$ approaches $M/4$. We can thus write an expression that gives us the upper limit of the term $\mu_{\sigma^2_{c_k|\varphi}}$:

$$\mu_{\sigma^2_{c_k|\varphi}} \le M\cdot\min\left(\frac{1}{4}, \frac{\sigma_n}{2\sqrt{\pi}}\right) \quad \text{..................(28)}$$

3.4. Variance of the conditional mean

The dependence of the term $\sigma^2_{\mu_{c_k|\varphi}}$ on the number of samples and the transition voltage is less monotone then the term $\mu_{\sigma^2_{c_k|\varphi}}$ (Figure 4).

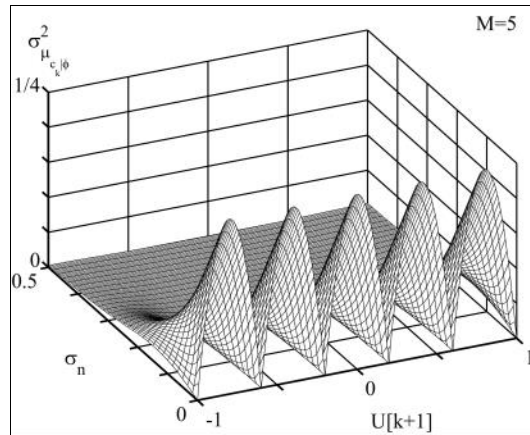

Figure 4 Representation of the term $\sigma^2_{\mu_{c_k|\varphi}}$ as a function of the normalized transition voltage ($U[k+1]$) and the input equivalent noise (σ_n).

For small values of the standard deviation of the noise the term $\sigma^2_{\mu_{c_k|\varphi}}$ depends strongly on the transition voltage. The number of arcs seen in Figure 4 is equal to the number of samples.

The maximum value of this term occurs in the absence of noise and it is equal to ¼.

3.5. Variance of the number of counts

The variance of the number of counts is determined by adding the terms $\mu_{\sigma^2_{c_k|\varphi}}$ and $\sigma^2_{\mu_{c_k|\varphi}}$ (Figure 5).

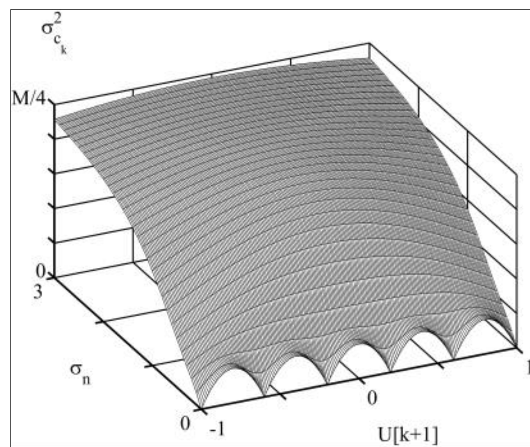

Figure 5 Representation of the term $\sigma^2_{c_k}$ as a function of the normalized transition voltage and of the standard deviation of the input-equivalent noise for the case of M = 5

Combining the conclusions from the two previous sections we reach the following expression for the upper limit of the variance of the number of counts.

$$\sigma^2_{c_k} \leq \max\left(\frac{1}{4}, M \cdot \min\left(\frac{1}{4}, \frac{\sigma_n}{2\sqrt{\pi}}\right)\right) \quad \text{.................(29)}$$

3.6. Variance of the transition voltages

The determination of the variance of the estimated transition voltages is, using (1) [11]:

$$\sigma_{T_k}^2 = \left(\frac{2A}{M}\right)^2 \sigma_{c_k}^2 \quad \text{..........(30)}$$

Inserting (29) leads to

$$\sigma_{T_k}^2 \le \left(\frac{2A}{M}\right)^2 \max\left(\frac{1}{4}, M \cdot \min\left(\frac{1}{4}, \frac{\sigma_n}{2\sqrt{\pi}}\right)\right) \quad \text{..........(31)}$$

4. Variance of the Code Bin Widths

4.1. Probability of a given sample belonging to a bin of the histogram

The code bin widths are computed from the histogram using (2). The analysis of the variance of the number of counts of the histogram is similar than the one presented for the cumulative histogram. The first difference is that the probability of a given sample belonging to a bin k of the histogram is given by

$$p_k(\gamma_j) = \int_{U[k]}^{U[k+1]} f_{u_j}(u \mid \gamma_j) \cdot du = \\ = \frac{1}{2} erf\left(\frac{U[k+1] + tri(\gamma_j)}{\sqrt{2} \cdot \sigma_n}\right) - \frac{1}{2} erf\left(\frac{U[k] + tri(\gamma_j)}{\sqrt{2} \cdot \sigma_n}\right) \quad \text{............(32)}$$

Instead of (10). This probability is depicted in Figure 6 as a function of sample phase, γ_j and input-equivalent noise standard deviation, σ_n.

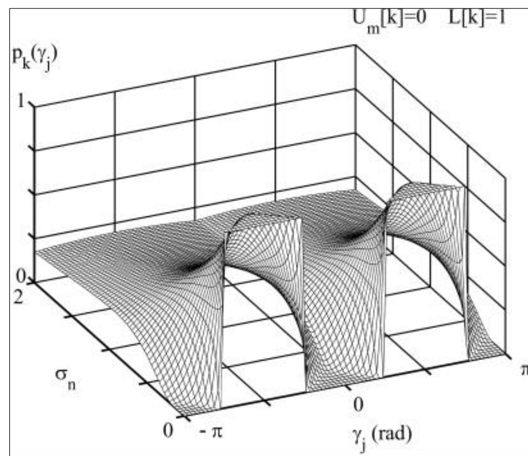

Figure 6 Representation of the probability that a sample belongs to a class of the histogram as a function of the sample phase (γ_j) and of the input-equivalent noise standard deviation (σ_n). Example with $U[k+1] = 0$ (transition voltage equal to the DC value of the stimulus signal)

Note that instead of using $U[k]$ and $U[k+1]$ it is easier to use the mean value of the normalized transition voltages and the code bin width given, in normalized units, by $U_m[k]$ and $L[k]$:

$$U_m[k] = \frac{U[k+1] + U[k]}{2} \quad , \quad L[k] = U[k+1] - U[k] \quad \text{..........(33)}$$

4.2. Mean of the conditional variance

The mean of the conditional variance of the number of counts of the histogram is obtained using (18) and (32). The result, as a function of the input-equivalent noise standard deviation and mean normalized transition voltage is depicted in Figure 7.

In Figure 8 the mean of the conditional variance is depicted as a function of the input-equivalent noise for a null mean transition voltage and a normalized code bin width of 0.02 (2% of the stimulus signal amplitude).

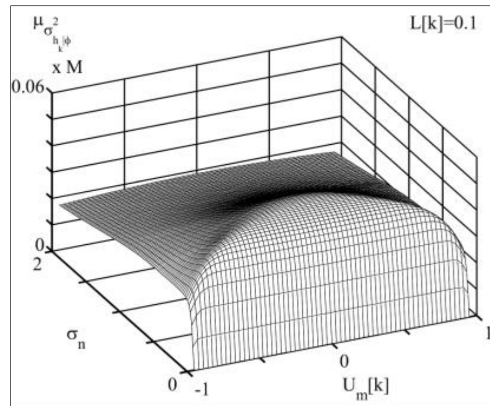

Figure 7 Representation of the term $\mu_{\sigma^2_{h_k|\varphi}}$ as a function of the standard deviation of the input-equivalent noise (σ_n) and of the normalized transition voltage

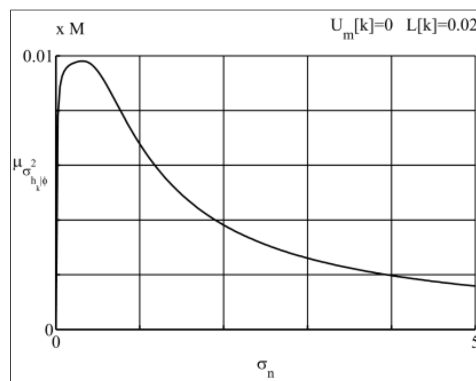

Figure 8 Representation of the term $\mu_{\sigma^2_{h_k|\varphi}}$ as a function of the standard deviation of the input-equivalent noise (σ_n)

Figure 9 depicts the same term for small values of noise standard deviation.

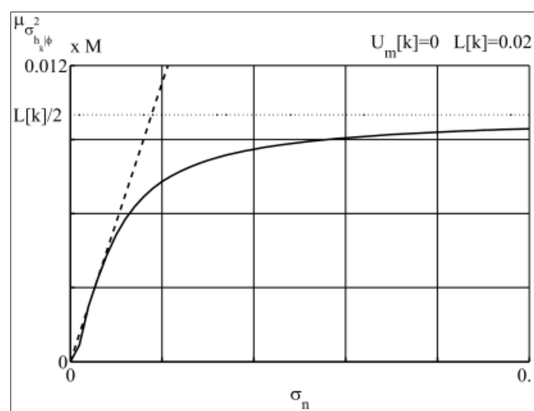

Figure 9 Representation of the term $\mu_{\sigma^2_{h_k|\varphi}}$ as a function of the standard deviation of the input-equivalent noise (σ_n). The dashed line represents the approximation for low values of noise standard deviation given by (34). The dotted line represents the maximum values attained by the mean of the conditional variance

When examining the impact of low noise standard deviation, it becomes evident that the mean behavior of the conditional variance closely approximates a straight line. To calculate the slope of this linear relationship, we can recall that the number of counts in bin k of the histogram is essentially the difference between the number of counts in bin k+1 and k of the cumulative histogram, as indicated in equation (3).

For situations with low noise standard deviation, the transition voltages (and correspondingly, the number of counts in the cumulative histogram) tend to become uncorrelated. Under these circumstances, the variance of the number of counts in the histogram is simply twice the variance of the number of counts in the cumulative histogram, as defined by equation (27):

$$\mu_{\sigma^2_{h_k|\varphi}} = \frac{M}{\sqrt{\pi}} \cdot \sigma_n \quad \text{................(34)}$$

This equation represents the dashed line in Figure 9. In Figure 8 and Figure 9 we can see that the mean of the conditional variance has a maximum of $L[k]/2$.

4.3. Variance of the conditional mean

The variance of the conditional mean of the histogram (Figure 10) has a similar behavior than it had in the case of the cumulative histogram (Figure 4).

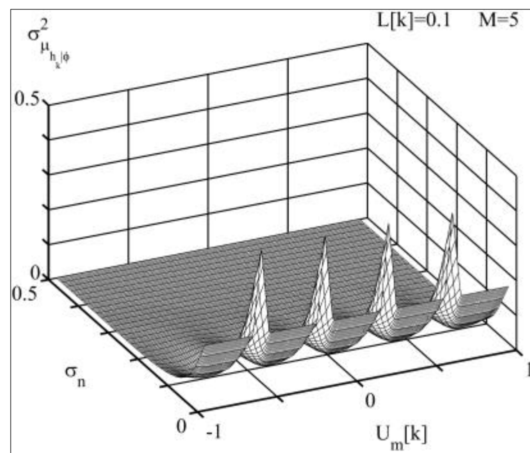

Figure 10 Representation of the term $\sigma^2_{\mu_{h_k|\varphi}}$ as a function of the normalized transition voltage ($U[k+1]$) and the input equivalent noise (σ_n)

In the case of the cumulative histogram, for small values of noise standard deviation, the variance of the conditional mean approached ¼. In this situation the number of counts in the cumulative histogram are uncorrelated and the variance of the number of counts of the histogram will be twice that of the cumulative histogram, that is, ½.

4.4. Variance of the number of counts

Using the conclusion that where reached in 4.2 and 4.3 we suggest the following expression for the upper limit of the number of counts of the histogram:

$$\sigma^2_{h_k} \le \max\left(\frac{1}{2}, \min\left(\frac{L[k]}{2}, \frac{\sigma_n}{\sqrt{\pi}} M\right)\right) \quad \text{..........(35)}$$

4.5. Variance of the code bin widths

The values of the code bin widths can be obtained directly from the number of counts of the histogram.

The variance of the code bin widths, considering (2), can thus be calculated by [25]

$$\sigma_W^2 = \left(\frac{2A}{M}\right)^2 \sigma_{h_k}^2 \qquad \text{……………(36)}$$

Substituting (35) in (36) leads to

$$\sigma_W^2 \leq \left(\frac{2A}{M}\right)^2 \max\left(\frac{1}{2}, \min\left(\frac{L[k]}{2}, \frac{\sigma_n}{\sqrt{\pi}} M\right)\right) \qquad \text{…………(37)}$$

5. Conclusion

In this research paper, we have successfully derived mathematical expressions that facilitate the precise determination of transition voltages and code bin widths for analog to digital converters (ADCs) tested with the Histogram Test Method using triangular stimulus signals. These expressions take into account the influence of input-equivalent random noise, both in the test setup and within the ADC itself. By incorporating these factors, we are able to compute an uncertainty interval for the estimates, adhering to modern measurement practices similar to those recommended in the Guide to the Expression of Uncertainty in Measurement (GUM). The intent of this uncertainty interval is to effectively express the quality and reliability of the measurements obtained during the ADC testing process.

As the Histogram Test Method involves a statistical approach where a considerable number of samples are acquired, it is crucial to optimize the test time by determining the minimum number of samples required. The mathematical expressions derived in this study play a pivotal role in calculating the necessary sample size, allowing us to minimize the testing duration without compromising the accuracy and validity of the results.

In summary, this paper not only provides valuable insight into accurately characterizing ADCs with the Histogram Test Method and triangular stimulus signals but also offers a means to evaluate and express the uncertainty in the obtained measurements. Additionally, the knowledge of the minimum required number of samples contributes to efficient testing practices, saving time and resources while maintaining the integrity of the testing process. These contributions collectively enhance the understanding and applicability of the Histogram Test Method for ADC characterization and promote the adoption of standardized and reliable testing methodologies in the field of electronics and signal processing.

Compliance with Ethical Standards

Acknowledgment

This work was supported in by Fundação para Ciência e a Tecnologia from Portugal under the research projects UIDB/50008/2020 and FCT.CPCA.2022.01 whose support the author gratefully acknowledges.

Disclosure of conflicts of interest

There are no conflicts of interest to report.

References

[1] IEEE std. 1057-1994, IEEE standard for digitizing waveform recorders, IEEE, Inc., New York, Dec. 1994.

[2] Blair J., Histogram Measurement of ADC Nonlinearities Using Sine Waves, IEEE Transactions on Instrumentation and Measurement, IM-43, pp. 373-383, 1994.

[3] Paolo Carbone and Giovanni Chiorboli, ADC Sinewave Histogram Testing with Quasi-choerent Sampling, Proceedings of the 17th IEEE IMTC Conference, vol. 1, pp. 108-113, May 2000, Baltimore, USA.

[4] F. Corrêa Alegria, A. Cruz Serra, Uncertainty in the ADC Transition Voltages Determined with the Histogram Method, Proceedings of the 6th Workshop on ADC Modeling and Testing, Lisbon, Portugal, September 13-14, 2001, pp. 28 32.

[5] F. Corrêa Alegria, A. Cruz Serra, Influence of Frequency Errors in the Variance of the Cumulative Histogram, IEEE Transactions on Instrumentation and Measurement, pp. 461-464, vol. 50, no 2, 2001, Publisher item identifier S 0018-9456(01)02972-2.

[6] F. Corrêa Alegria, A. Moschitta, P. Carbone, A. Cruz Serra, D. Petri, Effective ADC Linearity Testing Using Sinewaves, IEEE Transactions on Circuits and Systems, vol. 52. nº 7, pp. 1267-1275, July 2005.

[7] IEEE, "Standard 1057-1994 - IEEE Standard for Digitizing Waveform Recorders", December 1994.

[8] F. Corrêa Alegria, A. Cruz Serra, Uncertainty of the estimates of sine wave fitting of digital data in the presence of additive noise, 2006 IEEE Instrumentation and Measurement Technology Conference Proceedings, 24-25 April 2006, doi: 10.1109/IMTC.2006.328187.

[9] F. Corrêa Alegria, A. Cruz Serra, Gaussian jitter-induced bias of sine wave amplitude estimation using three-parameter sine fitting, IEEE Transactions on Instrumentation and Measurement, vol. 59, no. 9, September 2010, pp. 2328 2333, doi: 10.1109/TIM.2009.2034576.

[10] O. Birjukova, S. Guillén Ludeña, F. Corrêa Alegria, A. H. Cardoso, "Three dimensional flow field at confluent fixed-bed open channels", Proceedings of River Flow 2014, pp. 1007-1014, 2014, ISBN: 978-1-138-02674-2.

[11] O. Birjukova Canelas, R. M. L. Ferreira, S. Guillén-Ludeña, F. Corrêa Alegria, A. H. Cardoso, "Three-dimensional flow structure at fixed 70º open channel confluence with bed discordance", Journal of Hydraulic Research vol. 58 no. 3, pp. 434-446, 2020, doi: 10.1080/00221686.2019.1596988.

[12] S. Guillén-Ludeña, M. J Franca, F. Alegria, A.J. Schleiss, A.H. Cardoso, "Hydromorphodynamic effects of the width ratio and local tributary widening on discordant confluences", Geomorphology, vol. 293, pp. 289-304, September 2017, doi: 10.1016/j.geomorph.2017.06.006.

[13] F. Corrêa Alegria, P. Arpaia, P. Daponte and A. Cruz Serra, An ADC Histogram Test Based on Small-Amplitude Waves, Measurement, Elsevier Science, vol. 31, nº 4, pp. 271-279, June 2002.

[14] F. Corrêa Alegria, P. Arpaia, P. Daponte and A. Cruz Serra, ADC Histogram Test Using Small-Amplitude Input Waves, XVI IMEKO World Congress, Austria, vol. X, pp. 9-14, September 25-28, 2000.

[15] F. Corrêa Alegria, Pasquale Arpaia, Pasquale Daponte and António Cruz Serra, ADC Histogram Test by Triangular Small-Waves, IEEE Instrumentation and Measurement Technology Conference (IMTC), Budapest, Hungary, pp. 1690-1695, May 21-23, 2001.

[16] F. Corrêa Alegria, P. Arpaia, A. Cruz Serra and P. Daponte, Performance Analysis of an ADC Histogram Test Using Small Triangular Waves, IEEE Transactions on Instrumentation and Measurements, vol. 51, nº 4, pp. 723-729, August 2002.

[17] F. Corrêa Alegria and A. Cruz Serra, Overdrive in the standard histogram test of ADCs, Measurement, Elsevier Science, vol. 35, n. 4, pp. 381-387, June 2004.

[18] A. Cruz Serra, F. Corrêa Alegria, L. Michaeli, P. Michalko, J. Saliga, Fast ADC testing by repetitive histogram analysis, 2006 IEEE Instrumentation and Measurement Technology Conference Proceedings, pp. 1633-1638, Sorrento, Italy, 24-27, April 2006, doi: 10.1109/IMTC.2006.328161.

[19] F. Corrêa Alegria, A. Cruz Serra, Uncertainty of ADC random noise estimates obtained with the IEEE 1057 standard test, IEEE Transactions on Instrumentation and Measurement, vol. 54, no. 1, pp. 110-116, 2005, doi: 10.1109/TIM.2004.840226.

[20] S. Shariat-Panahi, F. Corrêa Alegria, A. Mànuel, A. Cruz Serra, IEEE 1057 jitter test of waveform recorders, IEEE Transactions on Instrumentation and Measurement, vol. 58, no. 7, 2234-2244, 2009, doi: 10.1109/TIM.2009.2013674.

[21] A. Cruz Serra, F. Corrêa Alegria, R. Martins and M. Fonseca da Silva, Analog-to-digital converter testing—new proposals, Computer Standards & Interfaces, vol. 26, nº 1, pp. 3-13, January 2004, doi: 10.1016/S0920-5489(03)00057-6.

[22] F. Corrêa Alegria, P. Girão, V. Haasz, A. Cruz Serra, Performance of Data Acquisition Systems from the User's Point of View, IEEE Transactions on Instrumentation and Measurement, vol. 53, nº 4, pp. 907-914, August 2004, doi: 10.1109/TIM.2004.830757.

[23] F. Corrêa Alegria, P. Girão, Vladimir Haasz and A. Cruz Serra, Performance of Data Acquisition Systems from User's Point of View, IEEE Instrumentation and Measurement Technology Conference, Vail, Colorado, USA, pp. 940-945, 20-22 May 2003.

[24] E. Martinho, F. Corrêa Alegria, A. Dionisio, C. Grangeia, F. Almeida, 3D resistivity imaging and distribution of water soluble salts in Portuguese Renaissance stone bas-reliefs, Engineering Geology, vol. 141, pp. 33 44, April 2012, doi: 10.1016/j.enggeo.2012.04.010.

[25] A. Papoulis, Probability, Random Variables and Stochastic Processes, McGraw-Hill, 3rd edition, 1991.